Transparent ZnO Resistive Switching Memory Fabricated by Neutral Oxygen Beam Treatment

Firman Mangasa Simanjuntak[1], Takeo Ohno[2]*, Kana Minami[2]*, and Seiji Samukawa[3]

[1]*Centre for Electronics Frontiers, University of Southampton, Southampton SO17 1BJ, United Kingdom*

[2]*Department of Engineering, Graduate School of Engineering, Oita University, Oita 870-1192, Japan*

[3]*Advanced Institute for Materials Research, Tohoku University, Sendai 980-8577, Japan*

E-mail: takeo-ohno@oita-u.ac.jp, v21e2009@oita-u.ac.jp

Abstract

In this work, we employed the Cu/ZnO/ITO resistive random access memory (RRAM) structure to investigate the effect of a neutral oxygen beam as a surface treatment for a ZnO film and its utility for the fabrication of RRAM devices. This treatment reduced the defect concentration in the sputtered-ZnO film and improves the resistive switching characteristics of the device. This result demonstrates the great potential of neutral oxygen beam for the development of RRAM devices.

1. Introduction

One of the next-generation non-volatile memories is a nanoionics resistive switching memory such as an atomic switch[1–3], memristor[4–5] and resistive random access memory (RRAM)[6–7], and its operating principle is based on an ionic conduction and electrochemical reaction. In the device structure, an oxide film is mainly used as a switching layer in which ion conduction occurs, and among them, research using zinc oxide (ZnO), which is a transparent material, is being actively conducted.

ZnO has been intensely investigated for various electronic applications in these recent decades.[8–11] However, the self-doped nature of ZnO material hinders the adoption of ZnO-based RRAM for the future data storage applications.[12] This nature results in high *n*-type conductivity; thus, ZnO-based RRAM has to be operated at high operation current in order to observe switching characteristics.

In previous work, we proposed a low-damage oxidation process using a neutral beam technique. The concept of this process, in which the kinetic energy of neutral oxygen (O) particles enables the formation of high-quality oxide films at low-temperature, is expected to be applicable to the oxidation of various materials. In fact, surface oxidation using the O beam can be applied for the formation of silicon (Si) oxide,[13–16] germanium oxide,[17,18] gallium arsenide oxide[19] and aluminum oxide.[20] In addition, formation of a tantalum oxide film and improvement of a ZnO film characteristic were reported to obtain a high quality metallic oxide films as an ionic transport layer, which was applied for the fabrication of RRAM devices, resulting in the typical bipolar resistive switching.[21–24] In this study, we investigate the effect of surface treatment by O beam on the ZnO film, and the electrical characteristics of ZnO-based RRAM where different treatment time of O beam were used.

2. Experimental methods

Figure 1 dipicts a generation system of the neutral O beam. This machine consists of an plasma chamber and an sample process chamber separated by a Si aperture electrode with numerous holes (aperture ratio: 50%) and a high aspect ratio (1mm in diameter and 10mm in length). In this system, O ions in the plasma can be efficiently neutralized by collision with the sidewalls of the aperture while passing through the holes. As a result, only neutral

O particles arrive at the sample, and the sample surface is treated by irradiation with a neutral O beam. The O plasma was generated using an inductively coupled plasma (ICP). Details of this system have been described elsewhere.[25,26)]

To investigate the electrical characteristics of RRAM, we fabricated copper (Cu)/ZnO/ITO structure shown in Fig. 2. ZnO thin films with a thickness of 23 nm were deposited onto a commercial indium tin oxide (ITO)-coated glass substrate using radio frequency sputtering. The ZnO films were irradiated with neutral O beam for various treatment time. The ICP plasma bias power, apearture bias power and O_2 gas flow were 2000 W, 40 W and 20 sccm, respectively. The sample temperature was room temperature. Surface treatment time with 0, 1, and 10 min of O beam were used. Hereafter, a 80-nm-thick Cu top electrodes were sputter-deposited using a metal shadow mask (with a diameter of 150 μm) onto the ZnO films.

Electrical characteristics were studied under atmospheric conditions using a semiconductor device parameter analyzer (Agilent B1500A) on a probe station; a voltage bias was employed on the top Cu electrode while the bottom ITO electrode was ground. Defect concentration in a ZnO film was evaluated using X-ray photoelectron spectroscopy (XPS; ULVAC-PHI Summitt XPS 1600). Crystal structure of the films were investigated using grazing incidence X-ray diffraction (GIXRD; Rigaku SmartLab 9MTP).

3. Results and discussion

Figure 3 shows the typical *R–V* characteristics of Cu/ZnO/ITO devices made with 0, 1, and 10 min of O beam treatment time. In the device, the ON state (low resistance state) is caused by the formation of a Cu metal filament between the Cu and ITO electrodes. In case of the 0-min device (as deposited), a resistance of less than 1 kΩ was obtained, and no switching behavior can be observed. This result means that a large leakage current of the sputtered-ZnO film is very high due to a thin film thickness of 23 nm. Conversely, obvious switching behaviors can be observed after the O beam treatment. Both 1-min and 10-min devices showed bipolar clockwise switching characteristic. Here, current compliance was employed during forming and set process to avoid permanent device breakdown. It is found that a 1 min of O beam treatment is sufficient to induce the switching curve with current compliance of 3 mA, while the switching behavior can even be observed at lower

current compliance of 1 mA by increasing the treatment time (10 min).

Figure 4 shows the *I–V* characteristics and the resulting pristine resistance of the Cu/ZnO/ITO device as a function of O beam treatment time. The resistance of the device without O beam treatment was 39.64 Ω, whereas it became 1796 and 7975 Ω after 1- and 10-min treatment, respectively. As expected, the pristine resistance of the devices made with longer treatment time exhibited higher resistance.

Figure 5 shows the endurance performance of the devices. The 1-min device indicated switching for more than 100 cycles with On/Off resistance ratio of 1 order of magnitude, as depicted in Fig. 5(a). Thus, the devices treated for 1 min showed stable switching, but unstable switching was exhibited after a long treatment time (Fig. 5(b)).

In general, a switching layer having a sufficient high resistivity is necessary to promote the formation of a conductive bridge; thus, a switching behavior can be observed. However, O vacancy is an intrinsic donor defect that plays a major role in the conductivity/resistivity of the ZnO film.[27] Therefore, a XPS analysis was conducted to evaluate the O vacancy in the ZnO film. Figure 6 shows a XPS spectrum of the O1s core level, and the obtained peak related to O ions in a deficient region was used to calculate a ratio of O vacancy and total oxygen.[28] As shown in Fig. 6(a), the O1s spectrum from the ZnO layer was fitted with three Gaussian peaks located at approximately 532.4 eV (O_{iii}), 531.05 eV (O_{ii}), and 530.25 eV (O_i). These peaks correspond to the amount of chemisorbed oxygen, the number of oxygens in the oxygen-deficient region, and the number of oxygens in the wurtzite structure of zinc ions surrounded by Zn atoms with a full complement of nearest-neighbor oxygen ions, respectively.[29] From the result of XPS, the amount of O vacancies in the surface region of the ZnO film were estimated, as shown in Fig. 6(b). Here, the O vacancy concentration was calculated by taking the ratio between the area of the O_{ii} peak and the total area of all O peaks ($O_{iii}+O_{ii}+O_i$). The O vacancy concentration at the surface of ZnO film decreased as the treatment time increases (the concentration decreases by more than 10% after 10-min-treatment). These results are consistent with the highest pristine resistance of the device with 10-min-treatment.

On the other hand, the switching characteristics of the device with a longer treatment time were poor. As shown in Fig. 5, the variation of resistance value in the endurance characteristics was smaller in the 1-min device than in the 10-min device. Figure 7 shows

GIXRD patterns of ZnO/ITO/glass samples with a different treatment time of O beam. Here, XRD analysis employing grazing incidence apparatus was conducted to investigate the grain growth of the surface of films. Although all of the GIXRD patterns are matched with wurtzite hexagonal structure, it was observed that the (002) orientation becomes less dominant while (101) orientation increases after the O beam treatment. It was also found that this decrease in (002) orientation did not change much between the devices irradiated for 1 min and those irradiated for 10 min. The grain having (002) orientation is beneficial for the formation of a confine Cu filament that leads to a stable switching due to its growth direction which is perpendicular to the substrate.[30,31] Therefore, it is considered that the reduction of (002) orientation causes unstable switching especially in the 10-min device due to the rejuvenation and rupture processes of the non-confine (branch or multi-) conductive bridge(s). Based on the above result, despite a 10-min treatment further improve the resistivity of the ZnO film, excessive irradiation of O beam leads to the increasing number of grain boundaries due to irradiation damage induce randomly oriented grains at the surface region of the ZnO film.

4. Conclusions

In summary, neutral O beam treatment is found effective to decrease O vacancy defects in the sputtered-ZnO film. The pristine resistance of the RRAM device increases as the treatment time increases; thus, it promotes the formation of the conducting filament at lower operation current. The results we obtained show the great potential of O beam treatment for the fabrication of oxide-based RRAM devices.

Acknowledgments

The authors acknowledge the experimental support from Mr. Kesami Saito for the film deposition and GIXRD characterizations.

References

1) K. Terabe, T. Hasegawa, T. Nakayama, and M. Aono, Nature **433**, 47 (2005).
2) T. Tsuruoka, K. Terabe, T. Hasegawa, and M. Aono, Nanotechnology **21**, 425205 (2010).
3) T. Ohno, T. Hasegawa, T. Tsuruoka, K. Terabe, J. K. Gimzewski, and M. Aono, Nat. Mater. **10**, 591 (2011).
4) D. B. Strukov, G. S. Snider, D. R. Stewart, and R. S. Williams, Nature **453**, 80 (2008).
5) G. Milano, M. Luebben, Z. Ma, R. D.-Borkowski, L. Boarino, C. F. Pirri, R. Waser, C. Ricciardi, and I. Valov, Nat. Commun. **9**, 5151 (2018).
6) H. Shima, F. Takano, and H. Akinaga, Appl. Phys. Lett. **91**, 012901 (2007).
7) M. Arita, Y. Ohno, Y. Murakami, K. Takamizawa, A. T.-Fukuchi, and Y. Takahashi, Nanoscale **8**, 14754 (2016).
8) L. S.-Mende and J. L. MacManus-Driscoll, Mater. Today **10**, 40 (2007).
9) D. Panda and T.-Y. Tseng, J. Mater. Sci. **48**, 6849 (2013).
10) F. M. Simanjuntak, T. Ohno, and S. Samukawa, AIP Advances **9**, 105216 (2019).
11) F. M. Simanjuntak, T. Ohno, and S. Samukawa, ACS Appl. Electron. Mater. **1**, 2184 (2019).
12) F. M. Simanjuntak, D. Panda, K.-H. Wei, and T.-Y. Tseng, Nanoscale Res. Lett. **11**, 368 (2016).
13) M. Yonemoto, T. Ikoma, K. Sano, K. Endo, T. Matsukawa, M. Masahara, and S. Samukawa, Jpn. J. Appl. Phys. **48**, 04C007 (2009).
14) A. Wada, K. Sano, M. Yonemoto, K. Endo, T. Matsukawa, M. Masahara, S.Yamasaki, and S. Samukawa, Jpn. J. Appl. Phys. **49**, 04DC17 (2010).
15) A. Wada, K. Endo, M. Masahara, C.-H. Huang, and S. Samukawa, Appl. Phys. Express **3**, 096502 (2010).
16) A. Wada, K. Endo, M. Masahara, C.-H. Huang, and S. Samukawa, Appl. Phys. Lett. **98**, 203111 (2011).
17) A. Wada, R. Zhang, S. Takagi, and S. Samukawa, Appl. Phys. Lett. **100**, 213108 (2012).
18) A. Wada, R. Zhang, S. Takagi, and S. Samukawa, Jpn. J. Appl. Phys. **51**, 125603 (2012).
19) C. Thomas, Y. Tamura, M. E. Syazwan, A. Higo, and S. Samukawa, J. Phys. D **47**, 215203 (2014).
20) T. Ohno, D. Nakayama, and S. Samukawa, Appl. Phys. Lett. **107**, 133107 (2015).

21) T. Ohno and S. Samukawa, Appl. Phys. Lett. **106**, 173110 (2015).

22) T. Ohno and S. Samukawa, Jpn. J. Appl. Phys. **55**, 06GJ01 (2016).

23) F. M. Simanjuntak, T. Ohno, and S. Samukawa, ACS Appl. Electron. Mater. **1**, 18 (2019).

24) F. M. Simanjuntak, T. Ohno, S. Chandrasekaran, T.-Y. Tseng, and S. Samukawa, Nanotechnology **31**, 26LT01 (2020).

25) T. Ohno, D. Nakayama, T. Okada, and S. Samukawa, Results Phys. **8**, 169, (2018).

26) S. Samukawa, Jpn. J. Appl. Phys. **45**, 2395 (2006).

27) F. M. Simanjuntak, O. K. Prasad, D. Panda, C.-A. Lin, T.-L. Tsai, K.-H. Wei, and T.-Y. Tseng, Appl. Phys. Lett. 108, 183506 (2016).

28) F. M. Simanjuntak, P. Singh, S. Chandrasekaran, F. J. Lumbantoruan, C.-C. Yang, C.-J. Huang, C.-C. Lin, and T.-Y. Tseng, Semicond. Sci. Technol. 32, 124003 (2017).

29) F. M. Simanjuntak, D. Panda, T.-L. Tsai, C.-A. Lin, K.-H. Wei, T.-Y. Tseng, J. Mater. Sci. **50**, 6961 (2015).

30) P. Singh, F. M. Simanjuntak, A. Kumar, and T.-Y. Tseng, Thin Solid Films **660**, 828 (2018).

31) F. Zhuge, S. Peng, C. He, X. Zhu, X. Chen, Y. Liu, and R.-W. Li, Nanotechnology **22**, 275204 (2011).

Figure Captions

Fig. 1. Schematic of the neutral oxygen beam system.

Fig. 2. Schematic of sample fabrication.

Fig. 3. Typical *R–V* curves of the Cu/ZnO/ITO devices while the O beam treatments for 0, 1 and 10 min were applied.

Fig. 4. Pristine resistance of Cu/ZnO/ITO devices made with different treatment time.

Fig. 5. Endurance performance of Cu/ZnO/ITO devices after O beam treatment for (a) 1 min and (b) 10 min.

Fig. 6. (a) XPS spectrum of O1s core level of O beam treated ZnO film and (b) O vacancy concentration on the ZnO surface as a function of O beam treatment time.

Fig. 7. Grazing-incidence XRD patterns of ZnO films having various treatment time.

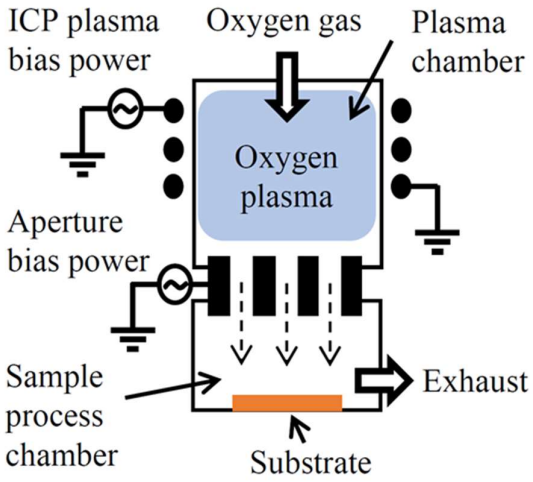

Fig. 1. Simanjuntak et al.

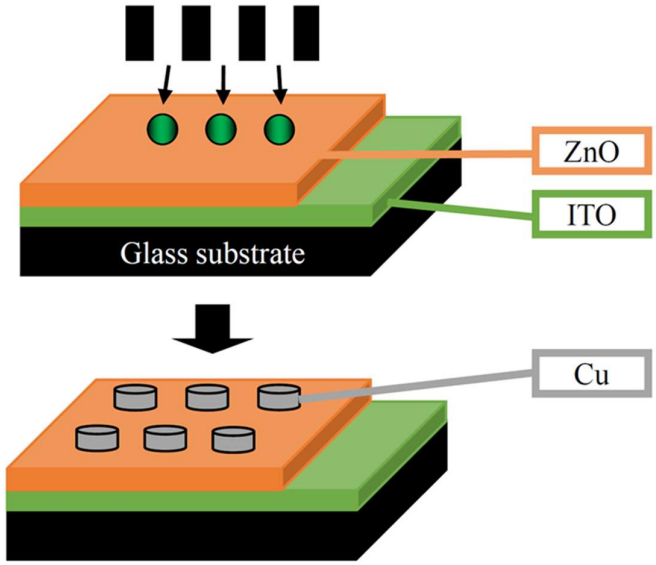

Fig. 2. Simanjuntak et al.

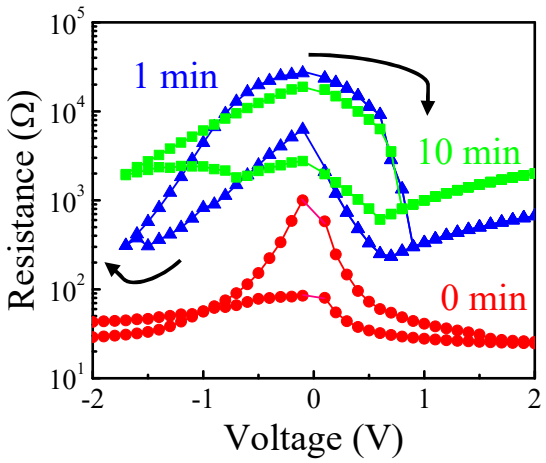

Fig. 3. Simanjuntak et al.

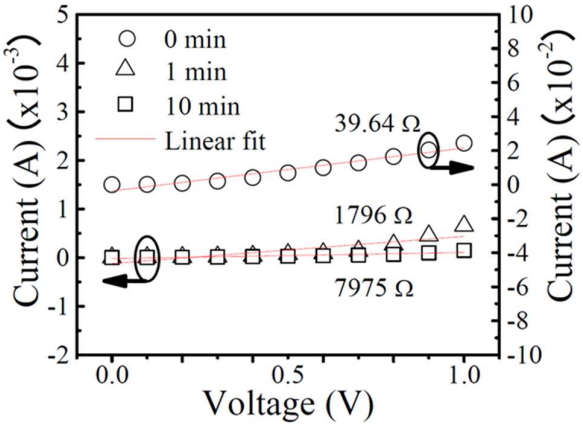

Fig. 4. Simanjuntak et al.

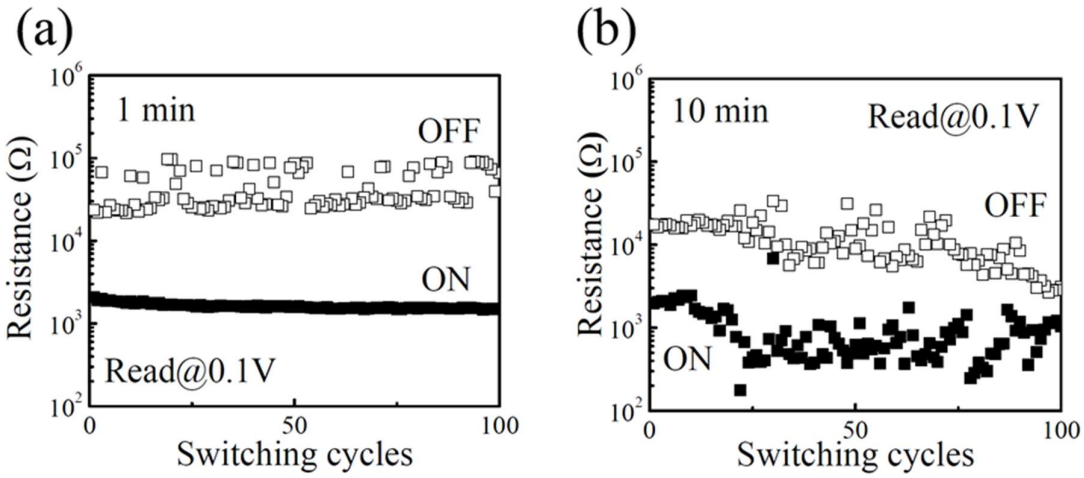

Fig. 5. Simanjuntak et al.

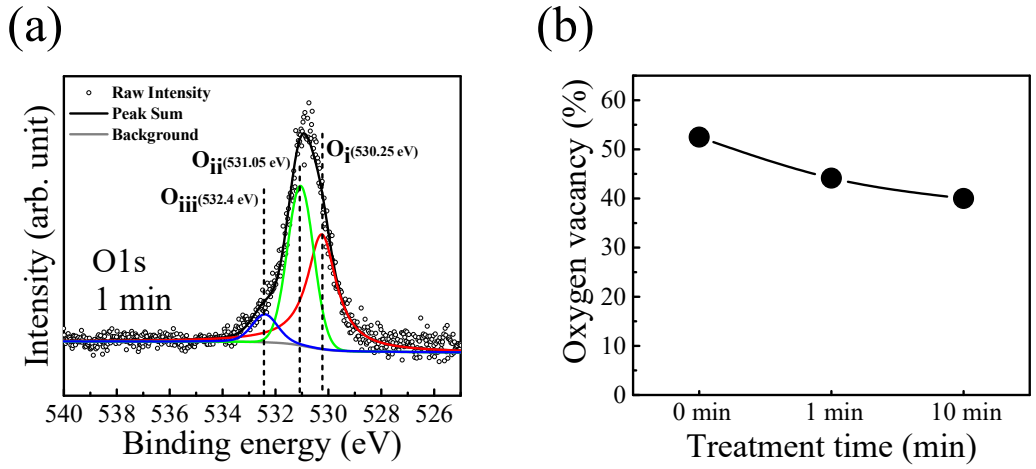

Fig. 6. Simanjuntak et al.

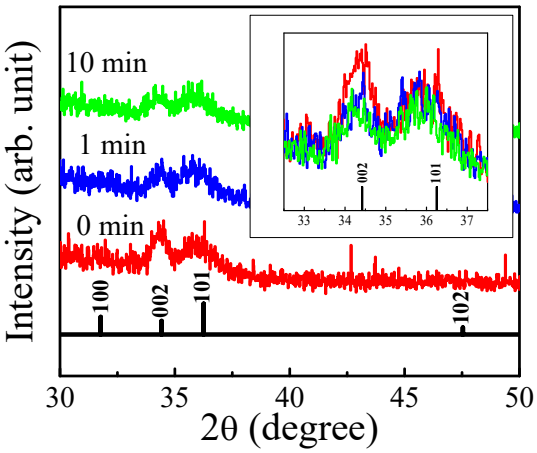

Fig. 7. Simanjuntak et al.